SUPPORTING INFORMATION

Regulating Ni oxidation states through ruthenium incorporation in Ni based catalysts

Laura Mallón,[1,‡] Laurent Peres,[2,‡] Nicolas Rivas,[3] Alba Garzón Manjón,[3,§] Marcos Gil-Sepulcre,[1,4] Olaf Rüdiger,[4] Serena DeBeer,[4] Nuria Romero,[2] Jérôme Esvan,[5] Jordi García-Antón,[1] Luis Rodríguez-Santiago,[6] Xavier Solans-Monfort,[6] Roger Bofill,[1] Karine Philippot,[2,*] Laia Francàs,[1,*] Xavier Sala[1,*]

‡ = equal contribution

[1] Departament de Química, Unitat de Química Inorgànica, Universitat Autònoma de Barcelona, 08193 Cerdanyola del Vallès (Barcelona), Spain. E-mail: laia.francas@uab.cat, xavier.sala@uab.cat

[2] CNRS, LCC (Laboratoire de Chimie de Coordination), UPR8241, University of Toulouse, UPS, INPT, Toulouse cedex 4 F-31077, France. E-mail: karine.philippot@lcc-toulouse.fr

[3] Max Planck Institute for Sustainable Materials GmbH, Max-Planck-Str. 1, 40237 Düsseldorf, Germany.

[4] Max Planck Institute for Chemical Energy Conversion, Stiftstrasse 34-36, D-45470 Mülheim an der Ruhr, Germany.

[5] Institut Carnot – Centre Inter-universitaire de Recherche et d'Ingénierie des Matériaux, INP-ENSIACET, CNRS, Université de Toulouse. 118, route de Narbonne, 31062 Toulouse, France.

[6] Departament de Química, Unitat de Química-Física, Universitat Autònoma de Barcelona, 08193 Cerdanyola del Vallès (Barcelona), Spain.

§ Current Address: Catalan Institute of Nanoscience and Nanotechnology (ICN2), CSIC and BIST, Campus UAB, Bellaterra, 08193 Barcelona, Catalonia, Spain.

Table S1. Overpotential and overpotential loss through Ru incorporation reported in the literature in comparison to the results of the present work.

Catalyst	η_{10} (mV) (pH 14)	$\Delta\eta_{10=}$Ni η_{10} – RuNi η_{10} (mV)	Ref
Ni-NW	454		This work
Ru(L)Ni-NW	414	40	This work
Ru(H)Ni-NW	476		This work
(Ru-Ni)Ox	237.2	125.9	1 (SA)
NiO	357.9		1 (SA)
Ru/D-NiFe*	189	61	2 (SA)
Ru/NiFe	223	27	2 (SA)
NiFe	250		2 (SA)
SR-Ru–NFO/NMO	229	29	3 (SA)
SR-NFO/NMO	258		3 (SA)
Ru_1Ni_1-NCNFs	290	50	4 (NPs)
Ni-NCNFs	340		4 (NPs)
RuO_2/NiO/NF	250	83	5 (NPs)
NiO/NF	333		5 (NPs)

Note that all the previously reported systems have directly doped NiO/Ni foam, which possesses higher surface area. SA = single atoms, NPs = nanoparticles.

*In this case an extra defect induction step has been carried out to generate oxygen vacancies.

1. Ru(HH)@Ni-NW characterization

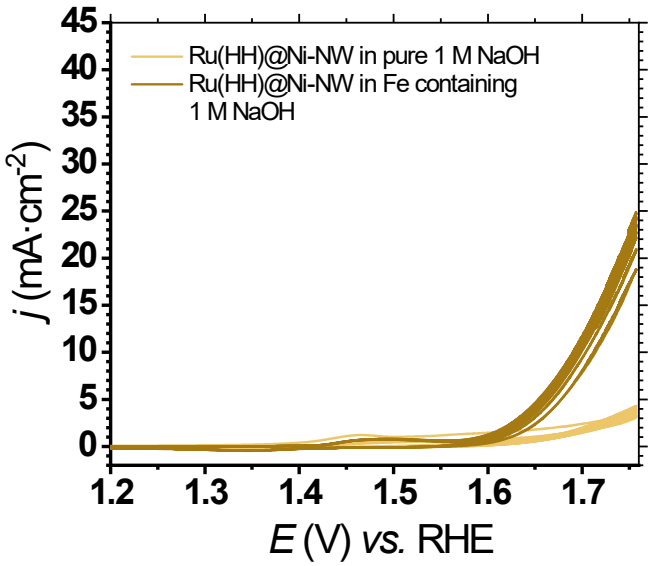

Figure S1. Consecutive CVs performed at pH 14 in Fe-free (purified) 1 M NaOH (light colours) and, afterwards, in Fe-containing (non-purified) 1 M NaOH (dark colours) to assess the OER electrocatalytic activity of **Ru(HH)@Ni-NW**.

2. Structural characterization

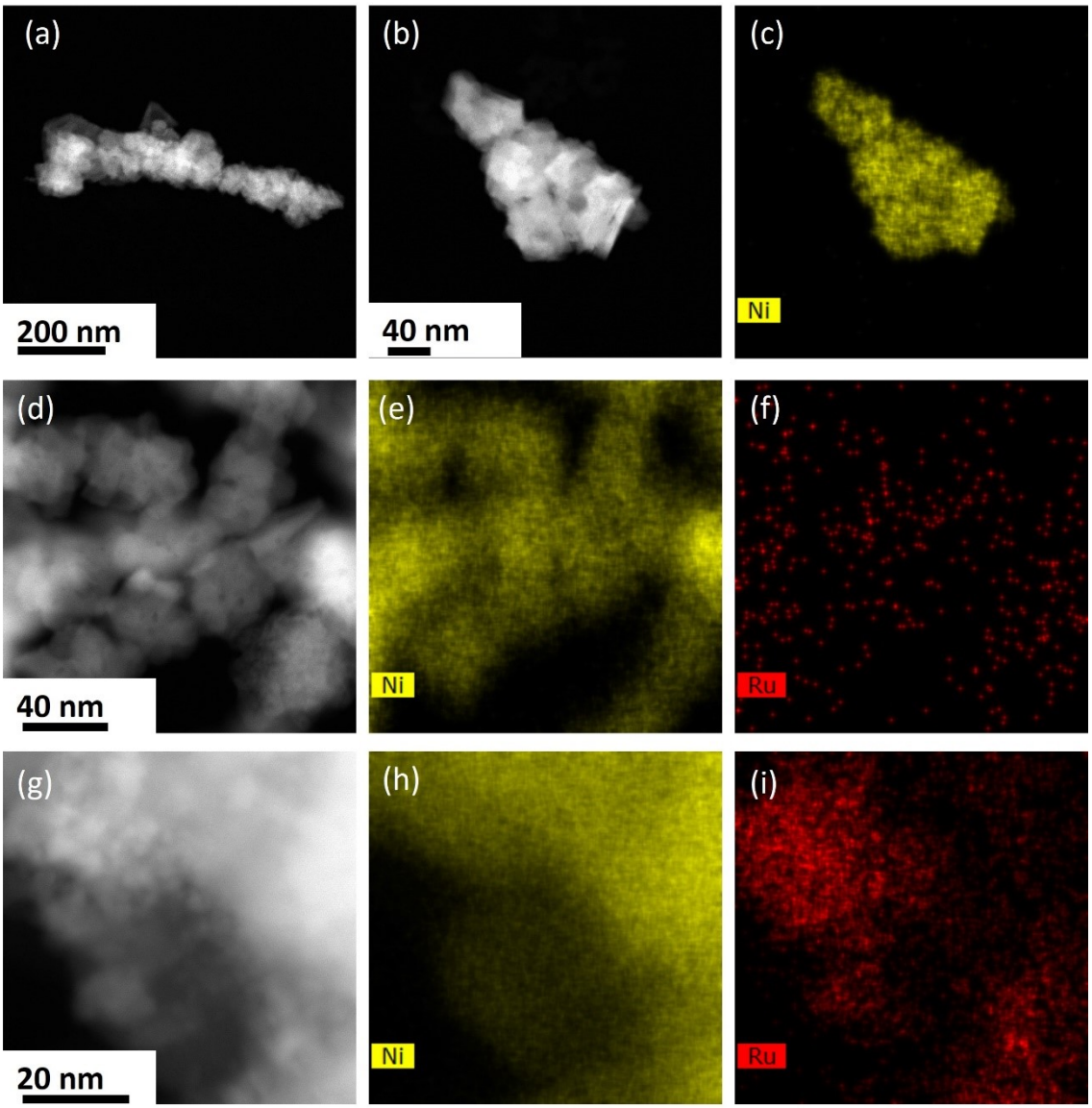

Figure S2. HAADF-STEM analysis and EDX mapping for **Ni-NW** (a-c), **Ru(L)@Ni-NW** (d-f) and **Ru(H)@-NW** (g-i).

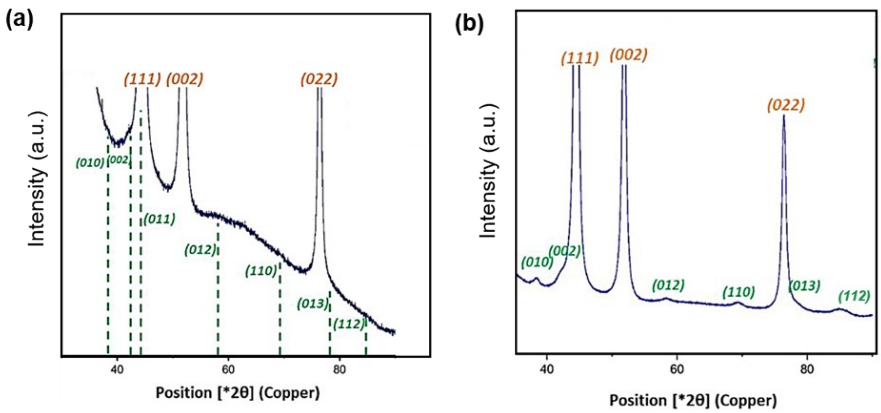

Figure S3. PXRD patterns for **Ru(L)@Ni-NW** (a) and **Ru(H)@Ni-NW** (b).

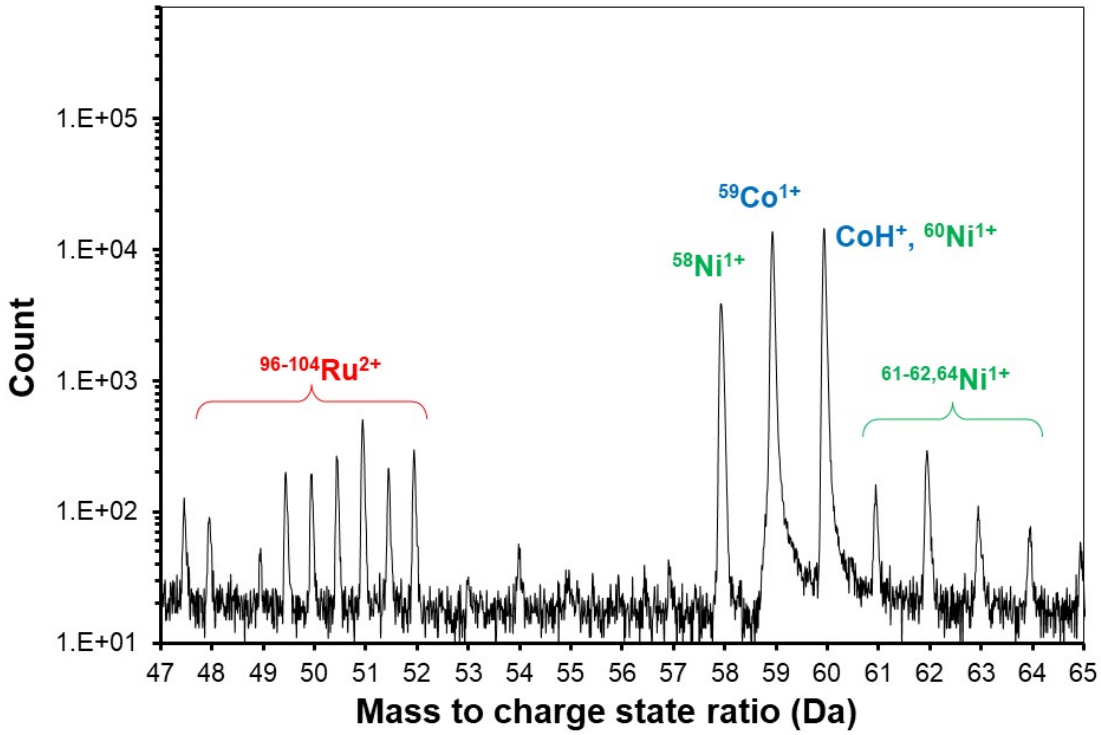

Figure S4. Representative mass spectrum between 47 and 65 Da obtained by APT for **Ru(L)@Ni-NW**. Major peaks are highlighted. Readily identifiable peaks at 48, 49, 49.5, 50, 50.5, 51 and 52 Da confirm the presence of Ru within the Ni NW, thanks to the low background level of the measurement (≈ 10 ppm). Additionally, the Ni peaks at 58, 60, 61, 62 and 64 Da were also detected. An overlap between the Co hydride that forms during field evaporation detected at 60 Da and the ^{60}Ni isotope is observable. Nonetheless, this does not affect the visualization or quantification of Ru in the sample.

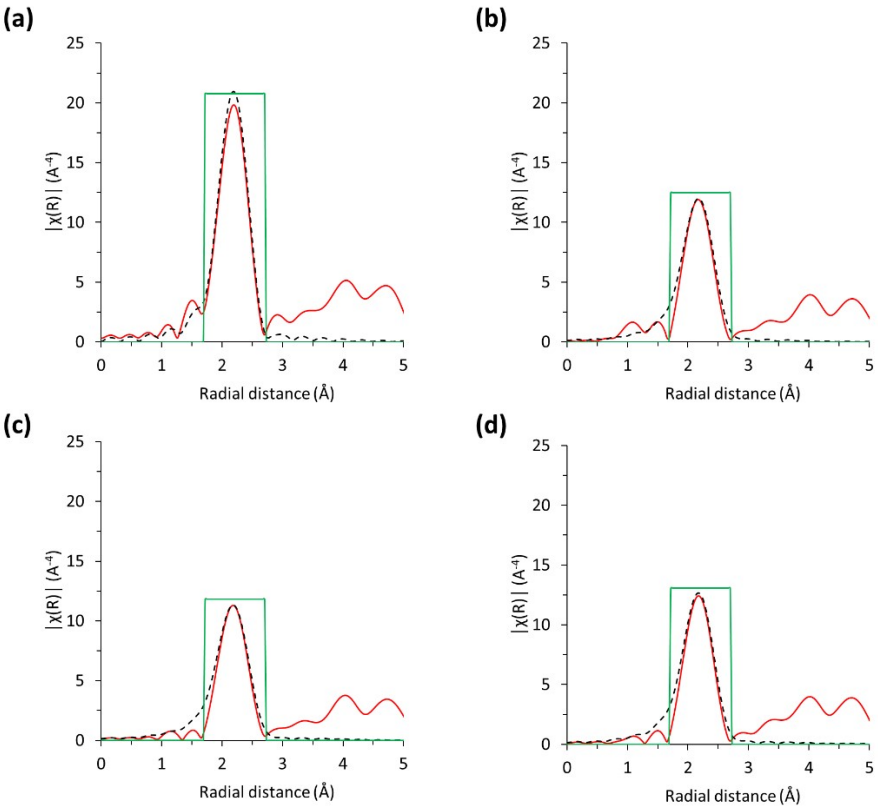

Figure S5. Plot of the k^3-weighted Ni EXAFS Fourier transform spectra for Ni(0) (a), **Ni-NW** (b), **Ru(L)@Ni-NW** (c) and **Ru(H)@Ni-NW** (d) nanomaterials. Experimental data are represented as solid red lines and the first shell fittings as black dashed lines. Experimental spectra were fitted over a k-range of 2–12 $Å^{-1}$.

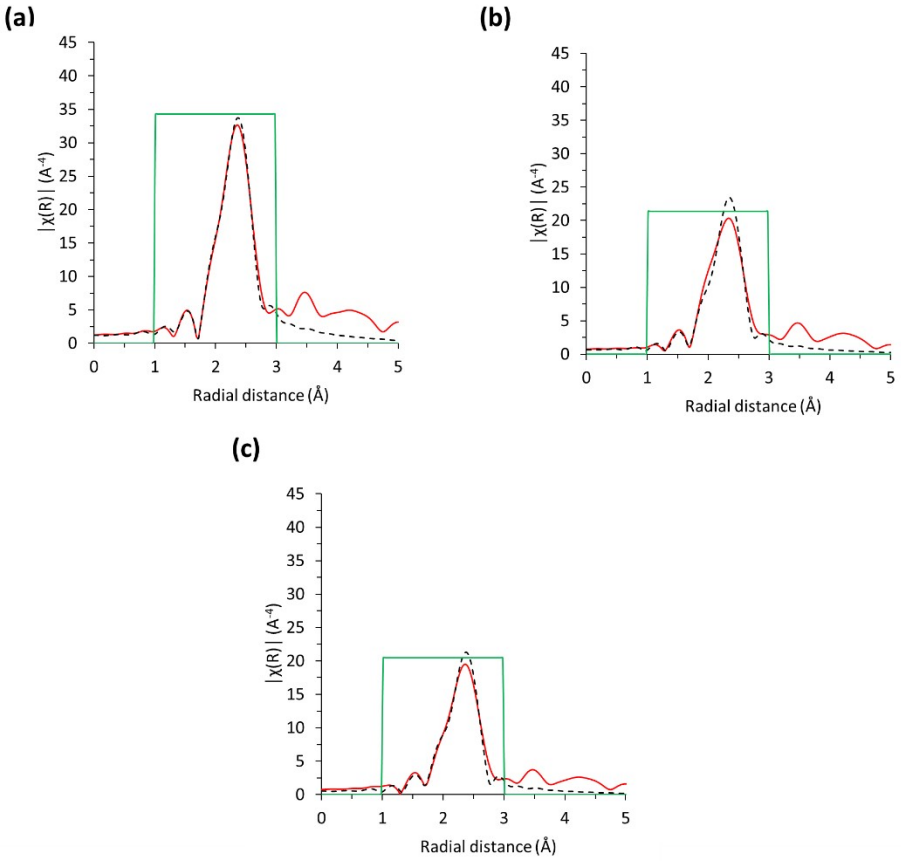

Figure S6. Plot of the k^3-weighted Ru EXAFS Fourier transform spectra for Ru(0) (a), **Ru(L)@Ni-NW** (b) and **Ru(H)@Ni-NW** (c) nanomaterials. Experimental data are represented as solid red lines and the first shell fittings as black dashed lines. Experimental spectra were fitted over a k-range of 2–12 $Å^{-1}$.

Table S2. EXAFS fitting parameters for Ni (top) and Ru (bottom).

Sample	Region	Shell, N	R, Å	σ^2 (10^{-3})	s^2	E_0,eV	R-factor	Reduced Chi-square
Ni(0)	k = 2 – 12 R = 1.7 – 2.7	Ni-Ni, 12	2.49	0.011	0.9	7.1	0.071	17377
Ni-NW	k = 2 – 12 R = 1.7 – 2.7	Ni-Ni, 12	2.49	0.016	0.9	6.6	0.272	1962
Ru(L)@Ni-NW	k = 2 – 12 R = 1.7 – 2.7	Ni-Ni, 12	2.49	0.016	0.9	6.8	0.279	1104
Ru(H)@Ni-NW	k = 2 – 12 R = 1.7 – 2.7	Ni-Ni, 12	2.49	0.016	0.9	6.6	0.241	861
Ru(0)	k = 2 – 12 R = 1 – 3	Ru-Ru, 12	2.68	0.005	0.9	-4.2	0.006	313
Ru(L)@Ni-NW	k = 2 – 12 R = 1 – 3	Ru-Ru, 12	2.67	0.007	0.9	-7.1	0.048	676
Ru(H)@Ni-NW	k = 2 – 12 R = 1 – 3	Ru-Ru, 12	2.68	0.007	0.9	-4.6	0.032	30

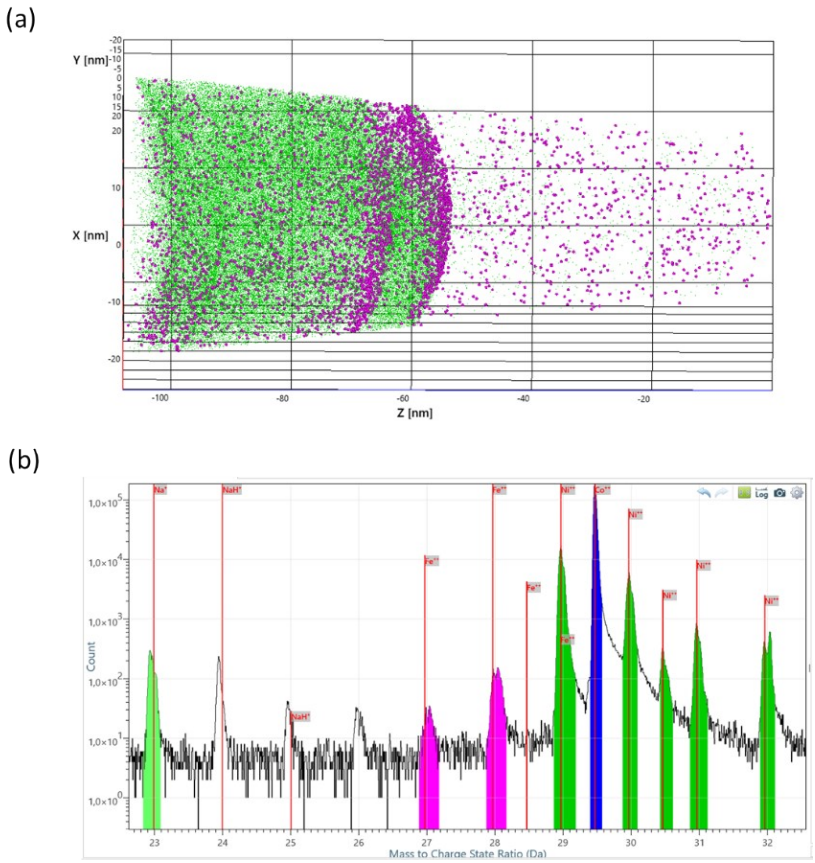

Figure S7. APT measurements on the **Ni-NW** nanomaterial after 24 h of stirring at pH 14 1 M NaOH unpurified electrolyte to study the Fe incorporation. Ni (green dots) and Fe (pink dots) distribution (a) and corresponding mass spectrum (b) are shown.

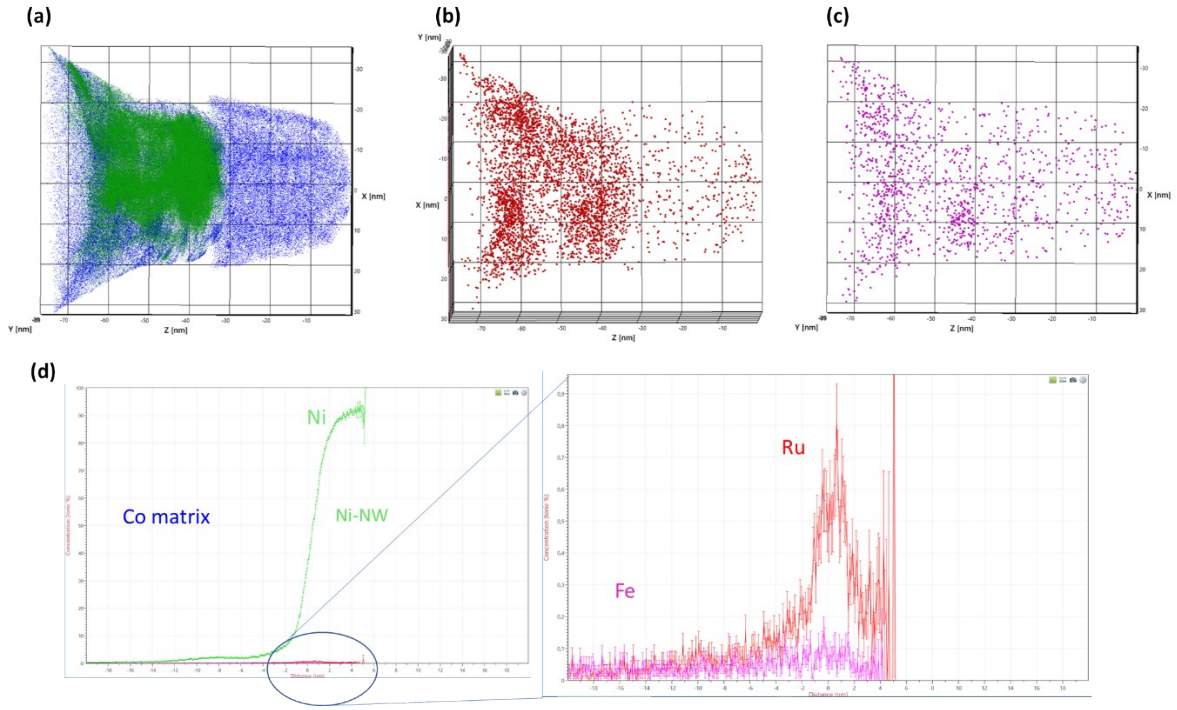

Figure S8. APT measurements on the **Ru(L)@Ni-NW** nanomaterial after 24 h of stirring at pH 14 1 M NaOH unpurified electrolyte to study the Fe incorporation. Ni (green) on the Co (green) tip distribution (a), Ru distribution (b), Fe distribution (c) and proximity histogram of the Ni iso-surface (d), where Ni foam stands for Ni-NW.

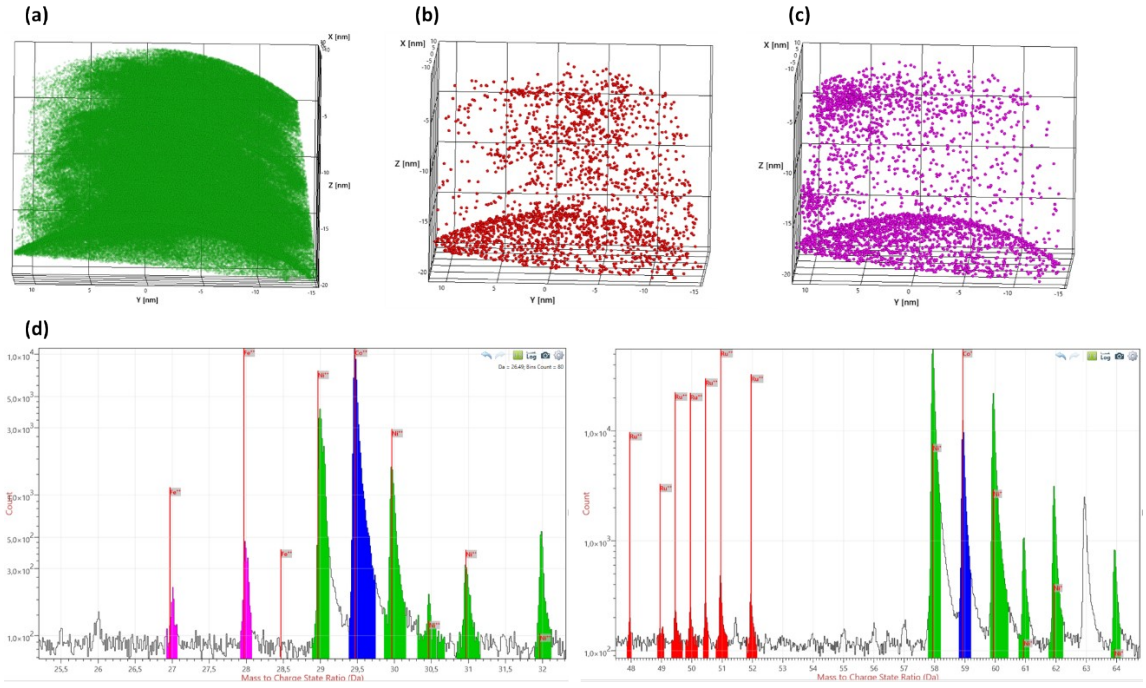

Figure S9. APT measurements on the **Ru(H)@Ni-NW** nanomaterial after 24 h of stirring at pH 14 1 M NaOH unpurified electrolyte to study the Fe incorporation. Ni distribution (a), Ru distribution (b), Fe distribution (c) and mass spectrometry analysis (d). MS color code: Fe, pink; Ru, red; Ni, green; Co, blue.

3. Long-term stability of Ru(L)@Ni-NW

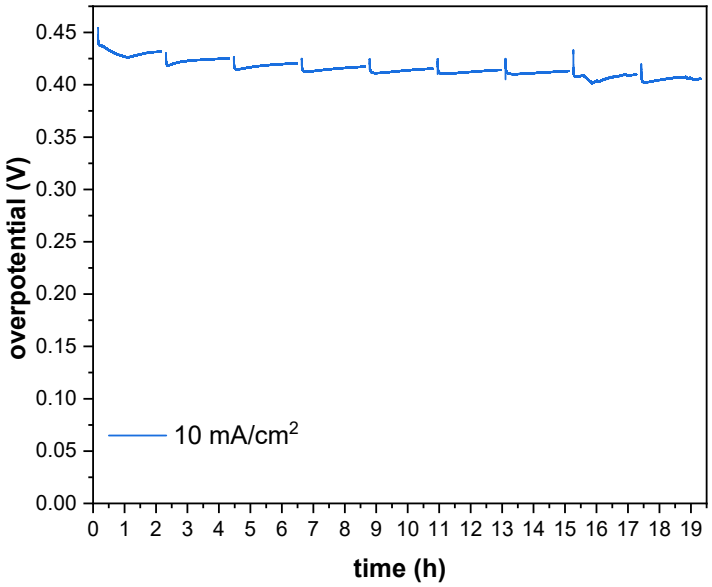

Figure S10. Chronopotentiometry at 10 mA/cm^2 for 19 hours of **Ru(L)@Ni-NW**.

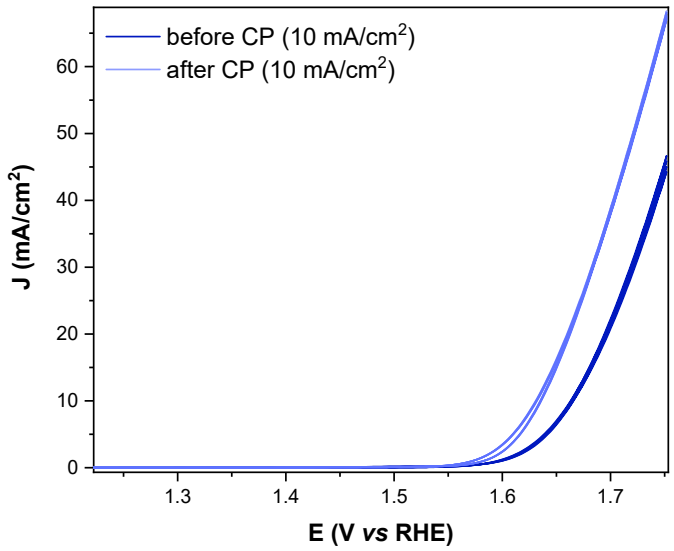

Figure S11. Ru(L)@Ni-NW CVs before (dark blue) and after (light blue) applying a 10 mA/cm^2 chronopotentiometry for 19 h.

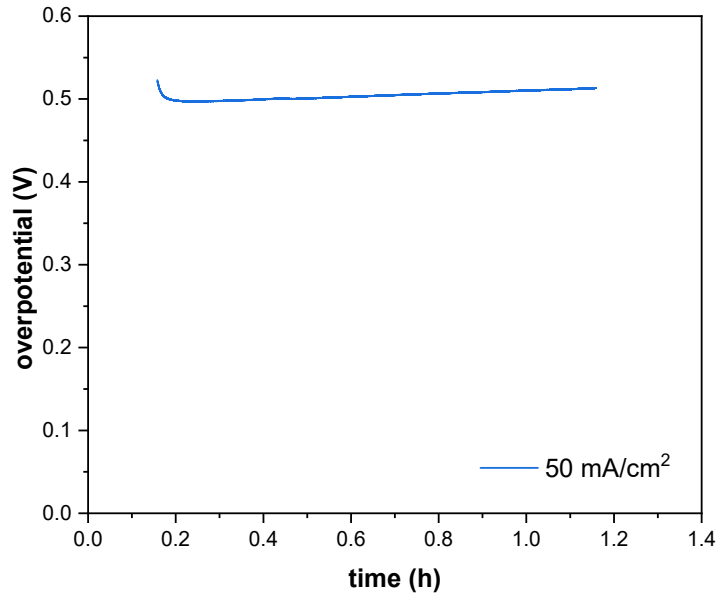

Figure S12. Chronopotentiometry at 50 mA/cm^2 for 1 hour of **Ru(L)@Ni-NW**.

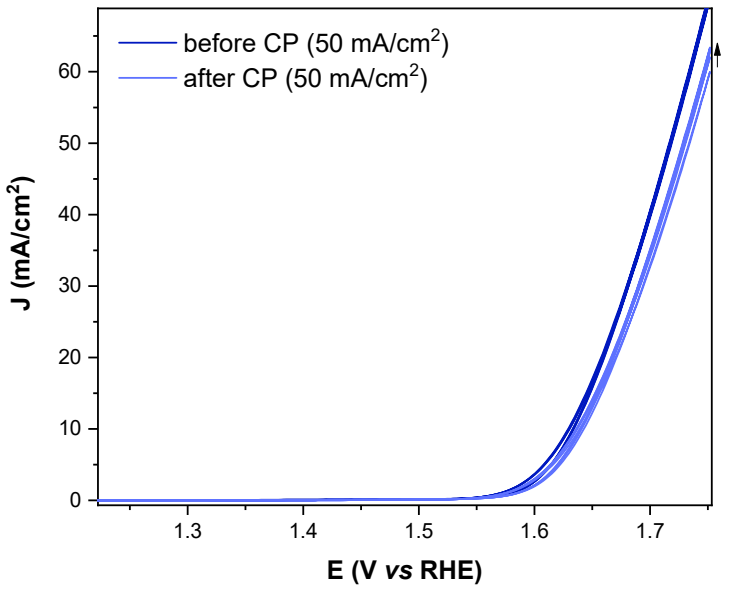

Figure S13. Ru(L)@Ni-NW CVs before (dark blue) and after (light blue) applying a 50 mA/cm^2 chronopotentiometry for 1h. The small arrow indicates the increasing current over consecutive CVs.

4. XPS analysis of Ru(L)@Ni-NW before and after OER testing

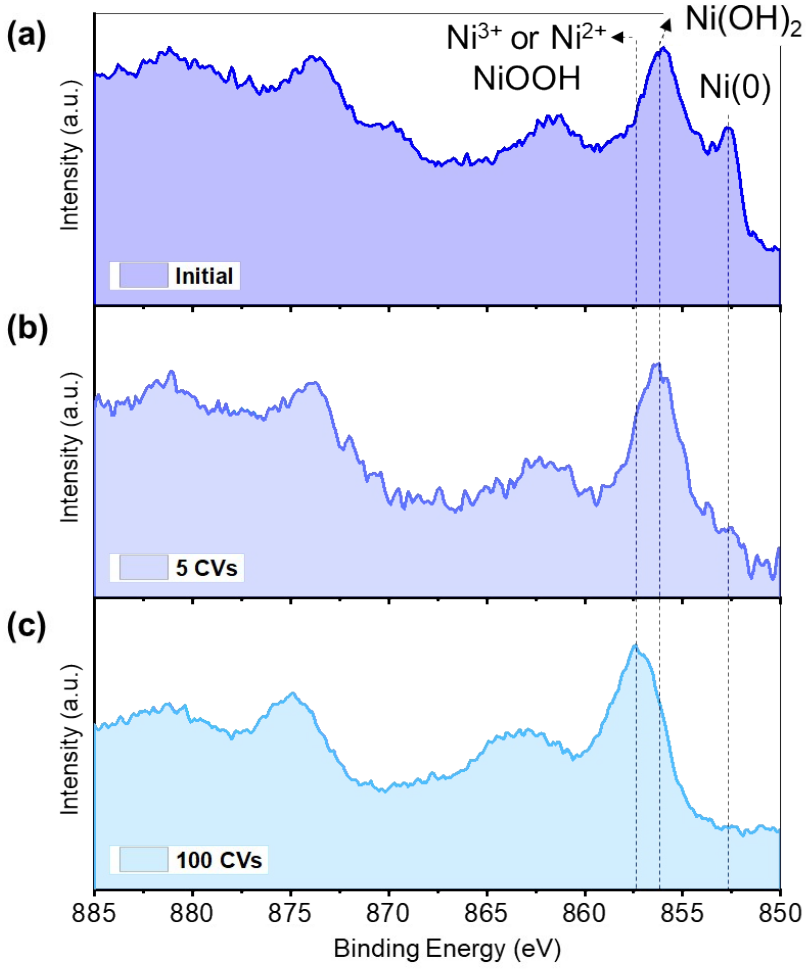

Figure S14. Ni 2p XPS spectra of **Ru(L)@Ni-NW** on FTO before OER catalysis (a) and after 5 (b) and 100 CVs (c).

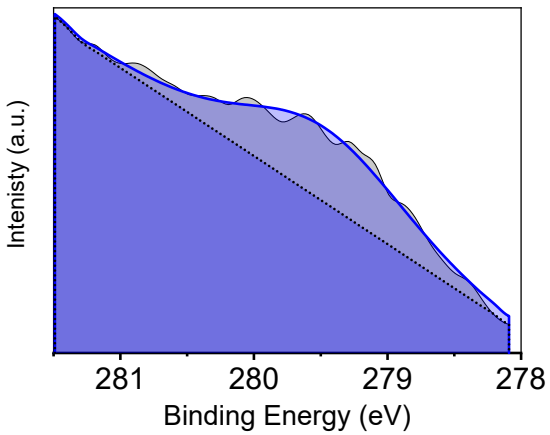

Figure S15. Ru $3d_{5/2}$ XPS spectra (279.7 - 280.3 eV) of an FTO electrode containing **Ru(L)@Ni-NW** after 24 h of stirring in 1 M NaOH (pH 14) unpurified electrolyte.

5. Spectroelectrochemical characterization

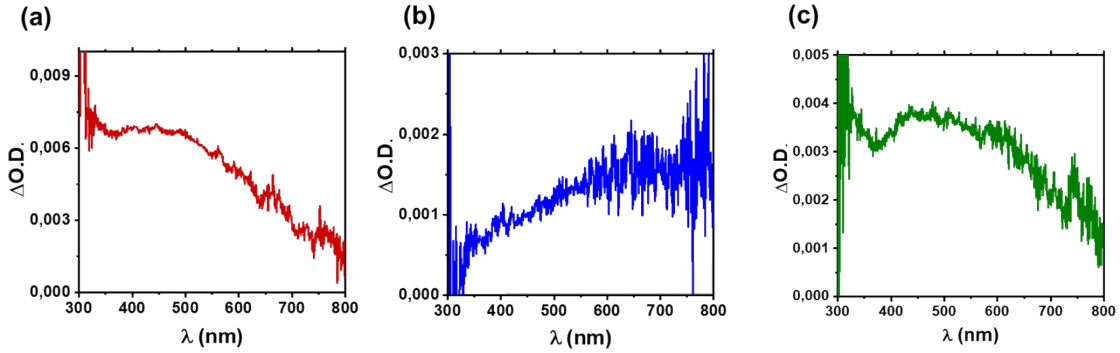

Figure S16. ΔO.D. spectra of the species accumulated after the Ni(II)/Ni(III) redox wave in Fe-containing 1 M NaOH electrolyte. **Ni-NW** (a), **Ru(L)@Ni-NW** (b) and **Ru(H)@Ni-NW** (c).

6. DFT calculations

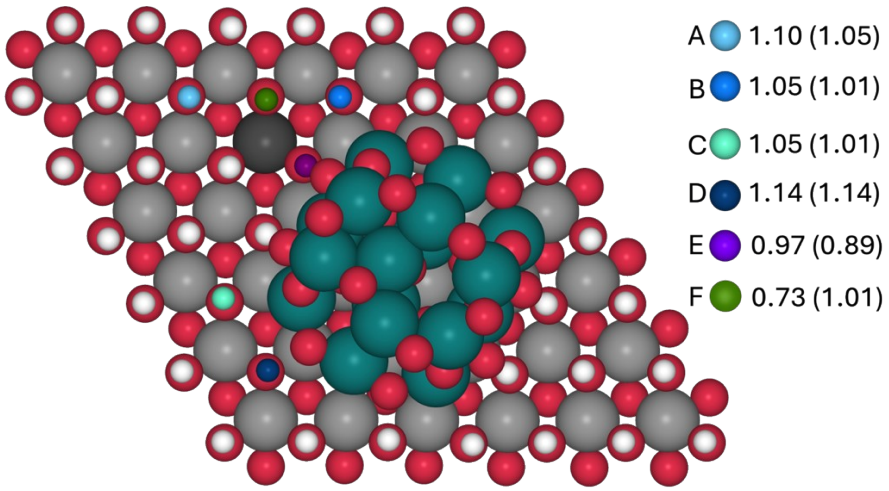

Figure S17. OH sites considered for the $Ni(OH)_2$ oxidation in the Fe (in black) containing $Ru_{17}O_{27}$ model and the corresponding computed potentials in V *vs.* RHE. Values in parenthesis correspond to the model without Fe.

7. References:

1 H. Zhang, Y. Lv, C. Chen, C. Lv, X. Wu, J. Guo and D. Jia, *Appl. Catal. B*, 2021, **298**, 120611.

2 P. Zhai, M. Xia, Y. Wu, G. Zhang, J. Gao, B. Zhang, S. Cao, Y. Zhang, Z. Li, Z. Fan, C. Wang, X. Zhang, J. T. Miller, L. Sun and J. Hou, *Nat. Commun.*, 2021, **12**, 4587. .

3 D. Kim, S. Park, J. Choi, Y. Piao, L. Yoon, S. Lee, D. Kim, L. Y. S. Lee, S. Park, Y. Piao and J. Choi, *Small*, 2024, **20**, 2304822.

4 M. Li, H. Wang, W. Zhu, W. Li, C. Wang, X. Lu, M. Li, W. Zhu, W. Li, C. Wang, X. G. Lu Alan MacDiarmid and H. Wang, *Adv. Sci.*, 2020, **7**, 1901833.

5 J. Liu, Y. Zheng, Y. Jiao, Z. Wang, Z. Lu, A. Vasileff and S. Z. Qiao, *Small*, 2018, **14**, 1704073.